Flexural-Torsional Response of FRP I-Section Members

Mojtaba B. Sirjani, Stella B. Bondi, and Zia Razzaq

***Abstract*—** Presented herein is the outcome of an experimental and theoretical study on Fiber Reinforced Plastic (FRP) beams with an I-shaped cross section subjected to four-point loading revealing the significance of lateral bending and warping strains due to practical imperfections. The paper also addresses the problem of combined bending and applied torsion. The results show that, for the case of combined bending and induced torsion, the sum of lateral and warping strains in FRP beams is not negligible even in the presence of only the in-plane or vertical loads. Based on measured strains, tentative strain-slenderness relationships are generated which account for the presence of lateral and warping strains in practical FRP beams. The effects of both induced and applied torsion combined with bending are explained with the help of numerical examples. It is also demonstrated that the boundary warping restraints in the form of member end plates cause a substantial decrease in the maximum warping normal stress in a torsionally loaded FRP member.

***Keywords*—** Beam buckling, experimental study, fiber reinforced plastic beams, FRP beam warping, lateral bending strain, load and resistance factor design, theoretical analysis, torsion, warping restraints

I. Introduction

A Fiber-Reinforced Plastic (FRP) beam subjected to in-plane bending moments about its cross-sectional strong axis can develop lateral-torsional buckling. In theory, such a beam will initially deflect normal to the strong axis until the critical value of the bending moment is reached where after lateral and torsional deflections develop. In real FRP beams, however, the vertical, lateral, and torsional displacements develop right from the start of the loading process, namely, as soon as the in-plane bending moments are applied, owing to even tiniest geometrical, material or loading imperfections. Thus, the actual beam also develops both lateral bending and warping normal strains. These strains are unaccounted-for in routine analysis and design procedures. In the present paper, the magnitude of these strains for such beams based on experiments is first summarized and discussed. The results are then used to develop tentative strain versus minor-axis (y-axis) slenderness ratio relationships for possible use in the analysis and design of FRP beams. The use of the proposed expressions for lateral bending and warping strain versus slenderness ratio expressions is demonstrated with a numerical example. The problem of combined bending and applied torsion is also addressed in this paper and the solution explained with the help of another numerical example.

Manuscript received Month October, 2011: Revised version received Month XX, YEAR.

M. B. Sirjani is with the School of Science and Technology, Norfolk State University, Norfolk, VA 23450 email: sirjani@nsu.edu

S. B. Bondi is with the Frank Batten School of Engineering and Technology, Engineering Technology, Old Dominion University, Norfolk, VA 23529 USA; phone 757-683-3775; fax 757-683-5655; email: sbondi@odu.edu

Z. Razzaq is with the Frank Batten School of Engineering and Technology, Civil and Environmental Engineering, Old Dominion University, Norfolk, VA 23529 USA email: zrazzaq@odu.edu

II. Problem Formulation

Figure 1 shows a FRP beam of length L and with an I-shaped cross section and subjected to a pair of gradually increasing applied loads each of magnitude *P*.

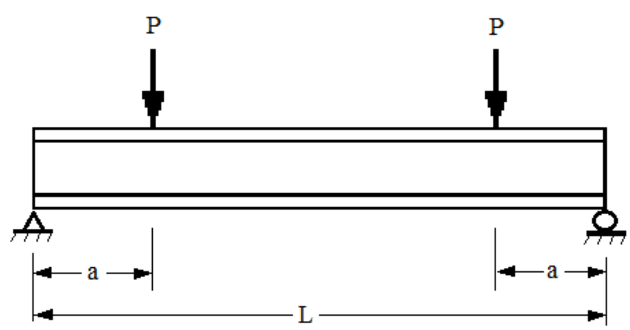

Figure 1. Beam and loading

III. Experimental Setup and Results

In an ideal or perfect beam, only vertical deflections (v) would develop initially until the beam either cracks, or develops lateral displacement (u) coupled with an angle of twist (β) corresponding to the lateral-torsional buckling load, Pcr. Experiments conducted by the authors on real FRP beams, however, showed that all three displacements (u, v, and β) developed as soon as the loads are applied, until the peak value of P is reached. The presence of lateral and torsional displacements of the type developed result in an increase in the total normal stress in the beam beyond that owing to just the in-plane bending effect. The problem is to develop a tentative practical analysis approach which may account for the presence of stresses associated with the lateral and torsional displacements in practical FRP beams. The problem of combined bending and applied torsion dealt with in this paper is schematically shown in Figure 2.

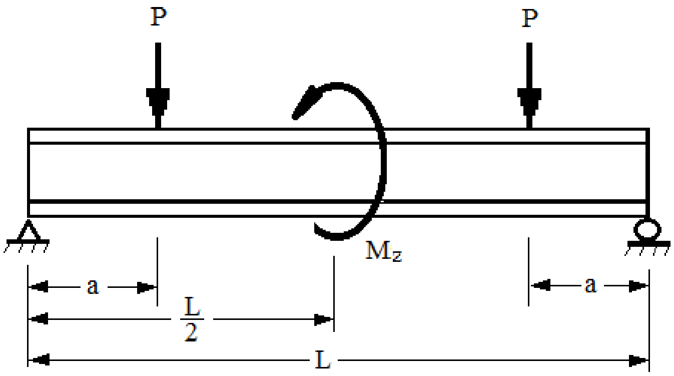

Figure 2. Combined Bending and Applied Torsion

Figure 3 shows the experimental test setup used for a series of FRP beams tested with the type of member geometry, loading, and boundary conditions schematically shown in Figure 1. As seen from Figure 3, the apparatus consists of several parts.

Figure 3. Experimental test setup used for a series of FRP beams

The beam supports consist of steel rods and angles which provide flexurally and torsionally simply-supported boundary conditions. A pair of round steel loading bars rest on the bottom surface of the beam flange, and the loading bars in turn is connected to vertical tie rod pairs of sufficient length so as not to constrain the lateral and torsional deflections when they develop. The top end of the tie rod pairs are connected to horizontal steel plates resting on a pair of load cells. The load cells are attached to the top of hydraulic jacks which react against a horizontal steel support cross-beam. As the load is gradually applied through the hydraulic jacks, the FRP beam deflects upward under the action of the load pair (*P*, *P*). As the load approaches the FRP beam capacity, significant lateral and torsional deflections begin to develop until the beam capacity is reached. At each load level, deflections and strains are recorded at key locations in the FRP member. Table 1 summarizes the experimental results based on five FRP beams with an I-shaped cross section (4 x 2 x 0.25 in.) and having lengths of 108, 96, 84, 72, and 60 inches. The table presents the applied load values and measured strains.

L (in.)	**P (lbs.)**	$\varepsilon_{u\beta}$ **x 10^{-6}**	ε_v	ε_t
	37	7	235	242
	48	16	302	318
108	61	29	409	438
	69	52	530	582
	71	97	605	702
	77	288	682	970
	37	1	121	122
	50	5	206	205
	66	7	290	297
96	77	15	361	376
	82	21	495	516
	101	46	616	662
	111	112	700	812
	29	12	63	75
	50	22	210	232
	82	38	327	365
84	93	66	432	498
	103	99	534	633
	114	156	630	786
	120	233	683	916
`	125	319	720	1039
	56	14	203	217
	78	32	301	333
	99	35	385	420
72	120	66	504	570
	141	91	651	742
	158	114	710	824
	177	184	816	1000
	190	354	892	1246
	120	25	381	406
	198	80	666	746
60	243	176	859	1035
	260	245	919	1164
	270	307	950	1257
	286	485	1001	1486
	292	795	1050	1845

Table 1. Summary of experimental results

The term $\varepsilon_{u\beta}$ represents the maximum sum of the lateral and warping flange tip strain, ε_v represents the maximum strain due to the in-plane bending effect, and ε_t is the total strain.

Figure 4 presents maximum strain versus the beam length plots.

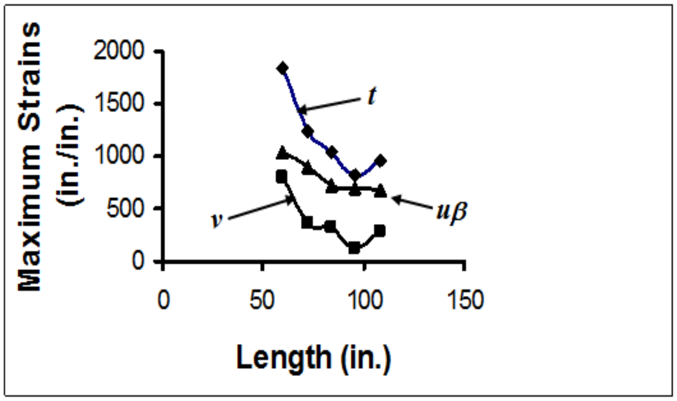

Figure 4. Maximum strains versus length

Figure 5 exhibits the relationship between the sum of the lateral and warping strains versus the beam minor-axis slenderness ratio. In this figure, the data point for the 96 in. long beam has been excluded in the curve-fitting process to arrive at a conservative relationship between the two variables.

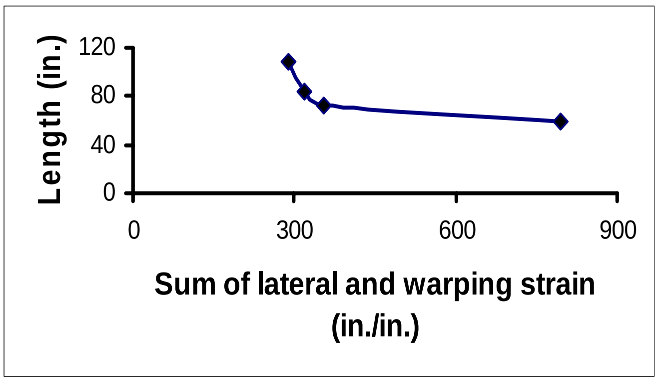

Figure 5. Length versus sum of lateral and warping strains

IV. Lateral Bending and Warping Strains

This ratio may become even much larger for some beams as demonstrated later in the paper by means of an example. Thus, in calculating the value of the maximum axial normal stress, the effect of the sum of the lateral bending and warping strains should not be neglected.

V. Experimental Strain versus Slenderness Relationships

Figure 3 demonstrates the relationship between $\varepsilon_{u\beta}$ and the minor-axis slenderness ratio, $\frac{L}{r_y}$, where r_y is the minor-axis radius of gyration. By approximating the curve in Figure 3 as a bilinear relationship, the following strain versus minor-axis slenderness ratio relationships are obtained corresponding to the beam maximum load, $P_{\max}$:

$$\varepsilon_{u\beta} = (-0.476\frac{L}{r_y} + 427.5)x10^{-6} \leq 208.75x10^{-6} \quad (1)$$

$$\varepsilon_{u\beta} = (-15.580\frac{L}{r_y} + 3000.0)x10^{-6} \geq 208.75x10^{-6} \quad (2)$$

Equating the strain expressions from Equations 1 and 2, and solving for $\frac{L}{r_y}$ results in defining the critical beam minor-axis slenderness ratio, $\frac{L_0}{r_y}$ = 171.04, which provides the demarcation basis between the two equations. Thus, the following analysis rules are generated:

If $\frac{L}{r_y} \geq \frac{L_0}{r_y}$ then Equation 1 is applicable.

If $\frac{L}{r_y} \leq \frac{L_0}{r_y}$ then Equation 2 is applicable.

The strain expressions presented herein are for the case of four-point loading and can tentatively be used to assess the strain values due to the induced lateral bending and torsional effects produced by practical imperfections in a FRP beam. Future research needs to be conducted to develop such expressions for various other types of loading and boundary conditions. The resulting expressions can provide a practical method for the analysis of FRP beams with a Load and Resistance Factor Design (LRFD) approach [1, 5-7].

The absolute value of the total maximum flange tip normal strain can be obtained by using the following expression:

$$\varepsilon_t = |\varepsilon_v| + |\varepsilon_{ub}| \quad (3)$$

The maximum normal stress can be computed using the following expression:

$$\sigma_t = E_{11}\varepsilon_t \leq \sigma_{cr} \quad (4)$$

in which E_{11} is the Young's modulus, and σ_{cr} is the FRP material cracking stress.

VI. Combined Bending and Induced Torsion: Example 1

Determine the total strain of a 6 x 3 x 0.25 in. I-section FRP beam with L = 144 in., end distance a = 20 in., load height above the cross section y_o^* = - 3.5 in., E_{11} = 2.53 x 10^6 psi, G_{12} = 0.42 x 10^6 psi, I_x = 15.872 in^4., I_y = 1.132 in^4., I_w = 9.2988 in^6., K_t = 0.6119 in^4.

Solution:

Referring to Figure 1, the beam buckling load can be found using the following formula [1] which is also applicable to I-section beams:

$$P_{cr} = \frac{0.5\left[-f_2 + \sqrt{f_2^2 + 4 f_1 f_3}\right]}{f_1} \qquad (5)$$

in which:

$$f_1 = \frac{1}{16}\left[f(a) - \frac{\pi^2 a^2}{L^2} - \frac{2\pi a}{l} g(a)\right]^2 \qquad (6)$$

$$f_2 = \frac{\pi^4 E_{11} I_y}{4L^3} y_0^* \sin^2\left(\frac{\pi a}{L}\right) \qquad (7)$$

$$f_3 = \frac{\pi^6 E_{11} I_y}{16L^4}\left[\frac{\pi^2 E_{11} I_w}{L^2} + G_{12} K_T\right] \qquad (8)$$

$$f(a) = \frac{\pi a}{L}\sin\left(\frac{2\pi a}{L}\right) - \sin^2\left(\frac{\pi a}{L}\right) \qquad (9)$$

$$g(a) = \frac{1}{2}\left[\pi\left(1 - \frac{2a}{L}\right) - \sin\pi\left(1 - \frac{2a}{L}\right)\right] \qquad (10)$$

Using the numerical values based on Equations 6 through 10 in Equation 5 gives the following buckling load:

P_{cr} = 376.0 *lbs*

For the service live load condition, the LRFD-based load factor is 1.6 [2]. Thus, the service load value of P is given by:

$$P = \frac{P_{cr}}{1.6}$$

Therefore:

P = 235.01 lbs.

The maximum in-plane bending stress is given by:

$$\sigma_b = \frac{Mc}{I_x} = \frac{Pac}{I_x}$$

which leads to:

$$\sigma_b = 888.39\, psi$$

Since $r_y = 0.6275$ in., the minor-axis slenderness ratio becomes:

$$\frac{L}{r_y} = 229.49 \geq 171.04$$

Therefore Equation 2 applies and gives:

$$\left|\varepsilon_{u\beta}\right| = 575.45x10^{-6}\,\frac{in.}{in.}$$

which results in the following normal stress due to this strain:

$$\sigma_{u\beta} = 1455.90\, psi$$

It is interesting to note that for this example, the normal stress due to induced lateral bending and warping is 1455.90 psi which far exceeds the primary bending stress of 888.39 psi. The absolute value of the total maximum flange tip normal stress equals:

$$\sigma_T = \sigma_b + \sigma_{u\beta} = 2344.29\, psi$$

For this specific beam, the predicted stress due to combined lateral bending and warping normal stress represents 62 percent of the total normal stress.

VII. Bending and Applied Torsion

For the member shown in Figure 2 with flexurally and torsionally pinned boundary conditions, the angle of twist, β, at any location Z along the member length due to a single concentrated torsional moment, M_z, can be shown to be equal to [3]:

$$\beta = Q_1\left[(1-\alpha)\frac{Z}{L} + Q_2\frac{a}{L}\sinh\frac{Z}{a}\right] \tag{11}$$

in which: Z = 0.5L and Z ≤L/2

$$\beta'' = Q_1\left[Q_2\frac{1}{aL}sinh\frac{Z}{a}\right] \tag{12}$$

in which:

$$Q_1 = \frac{ML}{GJ} \tag{13}$$

$$Q_2 = \left(\frac{\sinh\frac{\alpha L}{a}}{\tanh\frac{L}{a}}\right) - \cosh\frac{\alpha L}{a} \tag{14}$$

The warping normal stress, σ_w at the flange tips is given by [4]:

$$\sigma_w = E w_n \beta'' \tag{15}$$

in which, E is the modulus of Elasticity, w_n is the normalized unit warping, and β” is the second derivative of β. The analysis example given below demonstrates the procedure for finding the combined bending and normal stress for a FRP beam.

The warping shear stress is given by [4]:

$$\tau_w = - E\, S_w\, \beta''' \tag{16}$$

in which:

Sw is the warping statical moment at a point on cross section, given in in.^{4}, and β''' is given by:

$$\beta''' = Q_1\, Q_2\, \frac{1}{a^2 L} cosh\frac{Z}{a} \tag{17}$$

Equation (17) is applicable in the range $Z \leq L/2$.

For this example, the maximum value of β'' is found be at $Z = 0.5L$ using the third derivative of Equation (16). The resulting maximum warping shear stress based on Equation (17); however, with β''' based on torsionally fixed boundary conditions is found to be –54.39 psi. It is interesting to note that the corresponding maximum warping shear stress in the presence of torsionally pinned boundary conditions is found to be 6.37 x 10^{-6} psi using Equation (17). Thus, the presence of end warping restraints reduces the maximum warping shear stress by 9.6 percent.

VIII. Bending and Unrestrained Applied Torsion: Example 2

The beam in Example 1 is subjected to a pair of bending loads (P, P) as shown in Figure 2 as well as an applied midspan torsional moment of 300 lb-in. The boundary conditions are torsionally pinned, that is, the end cross sections are unrestrained relative to warping. Determine the total maximum normal stress in the beam including the effect of the warping normal stress due to the applied torsional moment. The maximum value of the normalized unit warping for the flange tip is 4.3125 in^2.

Solution:
Using Equations 13 and 14, we get:

Q_1 = 0.1680946

Q_2 = 5.3876 x 10^{-4}

Using Equation 12:

$\beta''_{z = 0.5L}$ = 0.6094556 x 10^{-4} rads./in.

Equation 15 gives the following warping normal flange tip stress the beam midspan as:

σ_w = 664.95 psi

The maximum bending stress for P = 235.01 lbs was found earlier in this paper as σ_b = 888.39 psi. The total normal stress is the sum of the bending stress plus the warping stress as given by:

$\sigma_{total} = \sigma_b + \sigma_w = 1{,}553.34$ psi

Thus, the warping stress is about 75% of the bending stress at the beam midspan. For these results to be valid, the maximum value of the midspan angle of twist, β, should be less than 6 degrees, which is a commonly accepted upper limit in structural engineering practice. For this example, β at midspan is found to be about 1.9 degrees. Therefore, the angle of twist is within the small deflection range.

For this example,

$$S_w = \frac{hb^2 t_f}{4} = 3.375 in.^4$$

where:

S_w = warping statical moment at a point on cross section, in.^{4}

h = beam depth center to center of flanges, in.

b = length of each cross-sectional element, in.

t_f = thickness of each cross sectional element, in.

Based on equation (17), the minimum value of $\beta'''=6.35 \times 10^{-6}$. This occurs at $Z = 0.5L$. The resulting warping shear stress based on equation (16) is found to be:

$\tau_w = -54.39$ psi

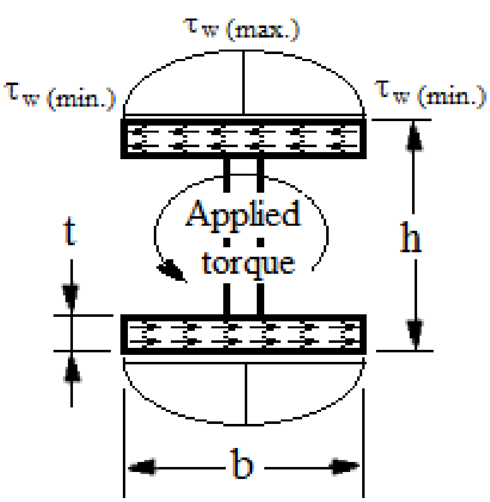

Figure 6. Cross-sectional of a beam with illustrated maximum warping stress.

Figure 6 illustrates the cross-sectional of a beam with applied torque that produces maximum warping stress.

IX. Free Versus Restrained End Warping: Example 3

For the member shown in Figure 6, the concentrated torque at $\alpha = 0.5$ with torsionally fixed end boundary conditions was used. At any location Z along the member length due to a single concentrated torsional moment, the angle of twist beta, β, can be obtained using the following expressions [3]:

In the range:

$$0 \le Z \le \alpha L$$

the angle of twist is given by:

$$\beta = \frac{Ma}{(H+1)GJ}\left\{\left[H \cdot \left\langle \frac{1}{sinh\frac{L}{a}} + sinh\frac{\alpha L}{a} - \frac{cosh\frac{\alpha L}{a}}{tanh\frac{L}{a}}\right\rangle + \right.\right.$$

$$\left.\left\langle sinh\frac{\alpha L}{a} - \frac{cosh\frac{\alpha L}{a}}{tanh\frac{L}{a}} + \frac{1}{tanh\frac{L}{a}}\right\rangle\right] \cdot$$

$$\left.\left[cosh\frac{Z}{a} - 1.0\right] - sinh\frac{Z}{a} + \frac{Z}{a}\right\} \tag{18}$$

In the range:

$$\alpha L \le Z \le L$$

the angle of twist is given by:

$$\beta = \frac{Ma}{(1+\frac{1}{H})GJ}\left\{\left[\frac{1}{H} \cdot \left\langle \frac{1}{sinh\frac{L}{a}} + cosh\frac{\alpha L}{a} - 1.0\right\rangle + \right.\right.$$

$$\left.\frac{\left(cosh\frac{\alpha L}{a} - cosh\frac{L}{a} + \frac{L}{a} * sinh\frac{L}{a}\right)}{sinh\frac{L}{a}}\right] +$$

$$cosh\frac{Z}{a}\left[\frac{1}{H} \cdot \frac{1}{tanh\frac{L}{a}}\left(1.0 - cosh\frac{\alpha L}{a}\right) + \right.$$

$$\left.\frac{\left(1.0 - cosh\frac{\alpha L}{a} \cdot cosh\frac{L}{a}\right)}{sinh\frac{L}{a}}\right] +$$

$$sinh\frac{Z}{a}\left[\frac{1}{H}\left(cosh\frac{\alpha L}{a} - 1.0\right) + cosh\frac{\alpha L}{a}\right] - \frac{Z}{a}\Bigg\} \tag{19}$$

where:

$$H = \left[\frac{1}{tanh\frac{L}{a}}\left(1.0 - cosh\frac{\alpha L}{a}\right) + \right.$$

$$\left.\frac{1}{sinh\frac{L}{a}}\left(cosh\frac{\alpha L}{a} - 1.0\right) + sinh\frac{\alpha L}{a} - \frac{\alpha L}{a}\right] /$$

$$\left[\frac{1}{sinh\frac{L}{a}}\left(cosh\frac{L}{a} + cosh\frac{\alpha L}{a} \cdot cosh\frac{L}{a} - cosh\frac{\alpha L}{a} - 1.0\right) + \right.$$

$$\left.\frac{L}{a}(\alpha - 1.0) - sinh\frac{\alpha L}{a}\right] \tag{20}$$

The above expressions are based on the solution of the governing differential equation of torsion for this case. Using Equation (12), it is found that the second derivative of the angle of twist, β'', at $Z = 0.5L$, takes the following form:

$$\beta'' = \frac{0.43M}{G_{12}K_t\Gamma} \tag{21}$$

where:

$$\Gamma = \sqrt{\frac{E\,I_w}{G_{12}\,K_t}} \tag{22}$$

If the end plates are absent, the resulting β'' expression becomes:

$$\beta'' = \frac{0.49M}{G_{12}K_t\Gamma} \tag{23}$$

Comparing the values of β'' from Equations (21) and (23) shows a 14 percent reduction in the member's midspan warping normal stress when end plates are added to the boundaries.

X. Conclusion

Experimental results show that the sum of lateral and warping strains in FRP beams is not negligible even in the presence of only the in-plane loads. Tentative strain-slenderness relationships are presented which account for the presence of lateral and warping strains in such beams due to real-life imperfections. The magnitude of the warping normal stress due to an applied torsional moment is of the same order of magnitude as that due to the primary bending loads. Furthermore, boundary warping restraints cause a substantial decrease in the maximum warping normal stress in a torsionally loaded member. The maximum warping shear stress is found to be relatively small.

References

[1] Razzaq, Z., Prabhakaran, R., and Sirjani, M.M., *"Load and Resistance Factor Design (LRFD) Approach for Reinforced Plastic Channel Beam Buckling,"* Structural Composites in Infrastructures Volume 27, Issues 3-4, 1996, Pages 361-369

[2] Load and Resistance Design Specification (LRFD), AISC, Chicago, IL, 2007.

[3] Torsional Analysis of Steel Members, AISC, Chicago, IL, 1983.

[4] Galambos, T.V., Structural Members and Frames, Prentice-Hall, Inc., Englewood Cliffs, New Jersey, 1968.

[5] Razzaq, Z., Khan, A. N., and Ali, S. M., "Effect of Warping Restraints on Lateral Torsional Buckling of FRP Beams," *Proceedings, 12th International Conference on Composites/Nano Engineering (ICCE/12)*, Tenerife, Spain, August 1-6, 2005.

[6] Sirjani, M. B., and Razzaq, Z., "Stability of FRP Beams under Three-point Loading and LRFD Approach," *Journal of Reinforced Plastics and Composites*, Vol. 24, No. 18, 2005.

[7] Sirjani, M. B., and Razzaq, Z., "Combined Biaxial Bending and Torsion of FRP I-Section Members at Cracking," *Proceedings, 14th International Conference on Composites/Nano Engineering (ICCE/14)*, Boulder, Colorado, July 2-8, 2006.

Mojtaba B. Sirjani was born in Mashhad Iran in 1959. He received a Bachelor's and a Master's degree in Mechanical Engineering from Old Dominion University, North Carolina State University in Mechanical Engineering, in 1984, 1989, respectively. Also, He received a Ph.D. in Civil Engineering from Old Dominion University in 1998.

He is currently a Professor in School of Science and Technology, Norfolk State University, and adjunct professor in the Department of Civil and Environmental Engineering, Old Dominion University, Virginia, USA. Before he selected academia as his career path, Dr. Sirjani has worked for two years in a consulting company as design structural engineer. Some of his publications include:
Sirjani, M.B., Bondi, S.B., Razzaq, Z. "Combined Bending with Induced or Applied Torsion of FRP I-Section Beams." *The 4th WSEAS International Conference on Engineering Mechanics, Structures, Engineering Geology (EMESEG '11)*, Corfu, Greece, EU, ISBN – 978-1-61804-022-0 pp. 358-363, July 14-17, 2011.

*Razzaq, z. Sirjani M.B.,"Bracing FRP I-Section Beams to Avoid Lateral Torsional Buckling"***,** The Journal of Reinforced Plastics and Composites, Sage International Journal Publication, Volume 30, NO 7, 557-560, April 2011.
Razzaq, Z. Sirjani, M.B., Prabhakaran, R.,*"LRFD Approach for FRP Channel Section Columns,"* The Journal of Reinforced Plastics and Composites, Sage International Journal Publication, (ISSN 0731-6844), Volume 28, Number 12, 2009.

Stella B. Bondi was born in Athens, Greece in 1955. Her undergraduate degree was in Civil Engineering and graduated from Old Dominion University, Norfolk, Virginia, USA in 1999. She continued her studies at Old Dominion University where she earned a Master in Engineering Management in 2003 and a PhD in Engineering Management in 2007, all from Old Dominion University.
She is an Assistant Professor at Frank Batten College of Engineering & Technology, Old Dominion University, Norfolk, Virginia, USA. Before she became an Assistant Professor, Dr. Bondi has worked for over 22 years in the consulting engineering industry.

Zia Razzaq was born in Pakistan in 1945. He received a Bachelor's, Master's, and a Doctoral degree in civil engineering from the University of Peshawar, Pakistan; University of Windsor, Canada; and Washington University, St. Louis, USA, in 1966, 1968, and 1974, respectively. He is currently a University Professor in the Department of Civil and Environmental Engineering, Old Dominion University, Virginia, USA.